

Are your **MRI contrast agents** cost-effective?

Learn more about generic **Gadolinium-Based Contrast Agents**.



**FRESENIUS
KABI**

caring for life

AJNR

Unilateral posterior arch fractures of the atlas.

R A Suss and K J Bundy

AJNR Am J Neuroradiol 1984, 5 (6) 783-786

<http://www.ajnr.org/content/5/6/783>

This information is current as
of April 19, 2024.

Unilateral Posterior Arch Fractures of the Atlas

Richard A. Suss¹
Kirk J. Bundy²

Unilateral posterior arch fractures of the atlas are discussed with two clinical examples and an experimental study of their mechanism. Laboratory fracturing of posterior arches of atlas specimens with a specially adapted universal testing machine produced nonsimultaneous fractures of the two sides in four of six specimens. In three of these specimens, a complete fracture on one side was temporarily displaced because the orientation of the leverage acting on the other side changed from sagittal to oblique. The consequent increase in the effective length of the lever arm reduced the angular deformation and strain on the second side. The second fracture occurred only after additional deflection of the posterior tubercle by up to 3 mm reproduced on the second side about the same angle of deformation that had caused the first fracture. A posterior arch fracture occurring by this mechanism will remain unilateral if the deflection is arrested before failure of the second side.

Although a major textbook [1] states that fractures of the posterior arch of the atlas (unassociated with fractures of other parts of the atlas) may be unilateral or bilateral, and Plaut [2] collected 10 reportedly unilateral examples among 99 atlas fractures of all types reviewed in 1938, we have found that the diagnosis of isolated unilateral posterior arch fracture has not won general acceptance among physicians. The objection raised has been that the atlas ring is a rigid structure that cannot be disrupted at just one point by the lever mechanism that causes posterior arch fractures. We present two clearly demonstrated clinical examples of isolated unilateral posterior arch fracture and describe a laboratory experiment showing that some bilateral fractures can occur sequentially, through a unilateral stage, rather than simultaneously.

Case Reports

Case 1

A 51-year-old man fell in a theater and was seen in an emergency room 12 hr later with neck pain. His neck was tender on the right in the region of the first cervical vertebra. A cervical spine series including flexion and extension views and computed tomography of the atlas demonstrated an isolated unilateral posterior arch fracture of the atlas on the right (fig. 1).

Case 2

A 17-year-old boy dived into shallow water and reportedly struck his forehead. He was seen in an emergency room 3 days later with pain in the back of his head and in his neck. No mark was visible on his forehead, and he did not recall the exact point of impact. Plain films and multidirectional tomography of the cervical spine and computed tomography of the atlas demonstrated an isolated unilateral posterior arch fracture of the atlas on the right (fig. 2).

Received February 2, 1984; accepted after revision April 19, 1984.

¹Russell H. Morgan Department of Radiology and Radiologic Science, Johns Hopkins Hospital, Baltimore, MD 21205. Present address: Department of Radiology, University of Texas Health Science Center at Dallas, 5323 Harry Hines Blvd., Dallas, TX 75235. Address reprint requests to R. A. Suss.

²Departments of Biomedical Engineering and Materials Science and Engineering, Johns Hopkins University, Baltimore, MD 21218. Present address: Department of Biomedical Engineering, School of Engineering, Tulane University, New Orleans, LA 70118.

AJNR 5:783-786, November/December 1984
0195-6108/84/0506-0783

© American Roentgen Ray Society

Materials and Methods

A universal testing machine (model TTDL, Instron Corp.), an apparatus used to test the strength of materials in tension or compression, was adapted for the application of a compressive force to an atlas specimen held in a vise (fig. 3). Ten uncleaned atlas vertebrae were obtained from adult cadavers that had been fixed in formaldehyde and phenol and used for instructional dissection. To permit their support in the vise, the atlas specimens' articular facets were trimmed and flattened with a bandsaw. Loading was applied through a $\frac{3}{16}$ -inch (4.8 mm)-diameter rod (fig. 3, *arrow*) placed in contact with the midpoint of the posterior arch so as to deflect the arch vertically. Since it has not been proven whether the usual force that produces posterior arch fractures is applied from above by the occipital bone or from below by the spinous process of the axis vertebra, some of the atlas specimens were fractured from above and some from below. Each atlas was advanced against the stationary rod at a constant rate of 3 mm/min in order to be able to resolve multiple fracture events while the applied load versus time was recorded on a strip chart recorder. When one side fractured first, deflection of the arch was continued until the other side fractured in order to measure the incremental deflection required to produce the second fracture.

Results

One specimen was sacrificed in a test of the apparatus. Two fractured through a sawn-off facet surface on one side because of inadequate support in the vise jaws. Another fractured initially in the midline at the point of contact with the rod. These four are not discussed further.

Of the remaining six specimens, two fractured on both sides of the posterior arch simultaneously (fig. 4A). The other

four fractured first on one side and then on the other. Three (specimens 1, 2, and 6) exhibited a sudden but incomplete decrease in loading associated with a sudden, visible, sideways tilting of the posterior arch (indicating unilateral fracturing and reorientation of leverage), followed after additional deflection by complete relief of loading as the second side fractured. Another (specimen 4) also underwent two-step fracturing but without developing a noticeable sideways tilt to the posterior arch, and was found to have bilateral greenstick fractures. The fractures in all six specimens traversed the vertebral artery sulci.

Three of the four asynchronously fractured atlas specimens exhibited a simple temporal pattern (fig. 4B) and one (specimen 6, the only one of the six that was loaded caudally and

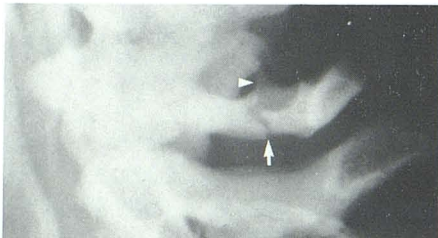


Fig. 1.—Case 1. One of four similar lateral cervical spine radiographs, each showing fracture through one side of posterior arch of atlas (*arrow*) and absence of fracture through other side, with unilateral ponticulus posticus intact (*arrowhead*).

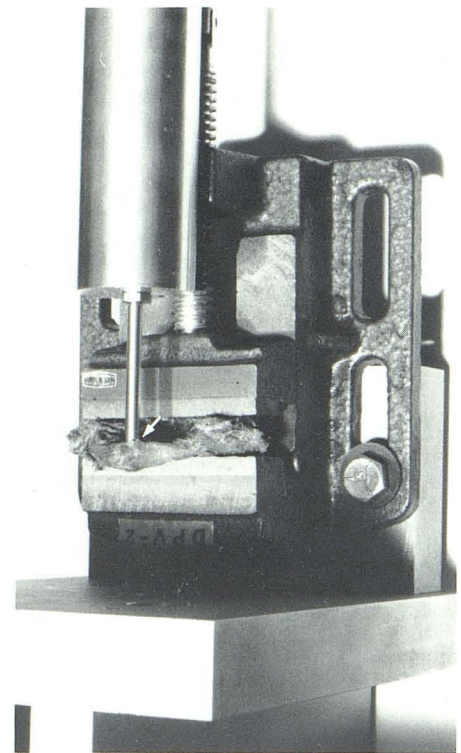


Fig. 3.—Universal testing machine containing vise and atlas specimen with midpoint of posterior arch apposed to rod (*arrow*).



Fig. 2.—Case 2. Lateral cervical spine multidirectional tomograms demonstrate posterior arch fracture of atlas on right (A) and no fracture on left (B). C, Thin-section (2 mm) computed tomogram of atlas shows isolated right posterior arch fracture. (Siemens DR3, window width 3000 H.)

Fig. 4.—Schematic drawings of graphs produced by six successfully fractured atlas specimens. **A**, Synchronous bilateral fractures in specimens 3 and 5. **B**, Simple pattern of asynchronous fractures in specimens 1, 2, and 4. **C**, Complex pattern in specimen 6 (with ponticulus posticus). Labeled points: a = onset of loading and angular deformation; b = peak load at first fracture; c = residual load immediately after first fracture; d = peak load at second fracture; e and f = additional events of load relief associated with complex fracture pattern on left side of specimen 6. *Broken lines* represent extrapolations to horizontal axis.

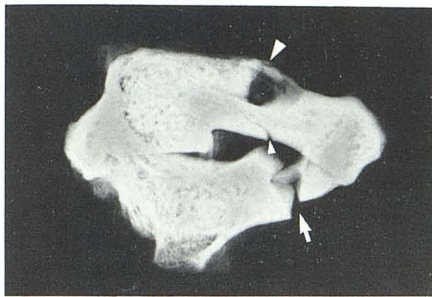
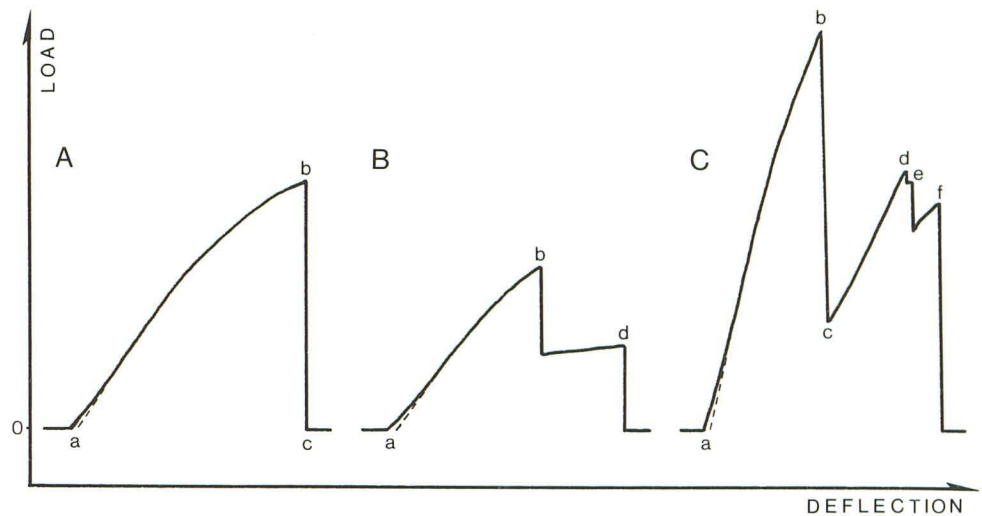


Fig. 5.—Tilted lateral radiograph of relatively massive atlas (specimen 6). Upward displacement of arch on right side at first fracture site (*arrow*) due to caudal loading, which was continued until left side fractured (undisplaced; *arrowheads*). Whereas bone is weaker under tension, ponticulus posticus on left side (*larger arrowhead*) was compressively loaded, explaining why this seemingly fragile structure did not fail before right side of arch.

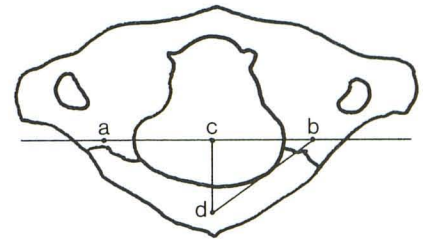
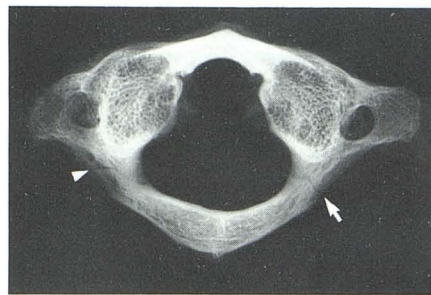


Fig. 6.—**A**, Radiograph of specimen 1 showing first (*arrowhead*) and second (*arrow*) fractures. **B**, Diagram for calculation of lever arms. Labeled lines and points: ab = fulcrum line in coronal plane through junctions of posterior arch with lateral masses; cd = length of lever arm (perpendicular to fulcrum line) during initial fracture; bd = length of lever arm during second fracture in specimens 1, 2, and 6.

the only one that had a ponticulus posticus) a more complex pattern (figs. 4C and 5) of load resistance in response to deflection. The maximum load borne by the posterior arch of each specimen at the time of the initial fracture varied widely, ranging from 15.3 to 74.5 kg (mean, 36.4 kg). For specimens, 1, 2, 4, and 6, the second-fracture maximum loads of 17.2, 16.1, 7.1, and 43.5 kg were 48.3%, 55.3%, 43.8%, and 58.4%, respectively, of the initial-fracture loads.

The deflections required for fracturing were analyzed trigonometrically. The length (L) of the effective lever arm (fig. 6, line cd or bd) from the point of contact with the rod to the fulcrum line in the coronal plane passing through the junctions of the posterior arch with the lateral masses (fig. 6, line ab) was measured on craniocaudal radiographs. The initial, sagittal (cd) lever arms were 15–18 mm long (mean, 15.7 mm) whereas the secondary, oblique (bd) lever-arm measurements for specimens 1, 2, and 6 were 26, 24, and 25 mm, respec-

tively. The deflection (D) of each posterior arch at the point of loading was calculated from the chart recording. Because of the likelihood of some initial settling of the specimens in the vise jaws (which would produce some measured loading without any actual deformation of the posterior arch or its junction with the lateral masses), when the initial part of the loading curve was upwardly concave the curve was extrapolated linearly from the point of inflection back to the horizontal axis. Deflection at the time of initial fracture varied from 2.2 to 4.9 mm (mean, 3.5 mm). The three specimens that fractured asynchronously and underwent lever-arm reorientation (specimens 1, 2, and 6) had incremental deflections of 2.8–3.0 mm between the first and second fractures, while the increment for specimen 4 was only 1.1 mm. Angular deformation was the induced vertical bending in the arch segment(s) constituting the lever, approximated as an angle at the fulcrum. The calculated angular deformation, $\arcsin(D/L)$,

existing at the time of initial fracture varied widely from 8° to 19° of arc in the six specimens, but in specimens 1, 2, and 6 the angles for the first and second fractures were within 2° of each other despite the change in length and orientation of the lever arm.

Discussion

Evans [3] has reviewed studies of the influences of the loading rate and various preservation treatments on the mechanical behavior of bone. As the loading rate decreases, the general effect both in tension and in compression is to decrease the stiffness of bone and to increase its ability to deform before fracturing. The quantitative effect, however, is only about twofold over a millionfold range of loading rates. Embalming increases resistance of bone to tension and decreases its resistance to compression, but again the effect is small, about 10%–20%. Therefore, although the experimental conditions did not exactly duplicate those present during injury in vivo, there is no reason to believe the differences were sufficient to invalidate our conclusions about the fracture mechanism.

The production of asynchronous fractures by a directly vertical, midline force vector refutes the assumption of Plaut [2] that an asynchronous or asymmetric fracture of the posterior arch can be produced only by an obliquely applied force. Because no structure is perfectly symmetric or histologically uniform, one side of the posterior arch must begin to fail slightly before the other. Although a unilateral ponticulus

posticus buttressing its side may contribute to the inherent asymmetry of the arch, specimens 1, 2, and 4 and case 2 demonstrate that a gross asymmetry is not required for asynchronous fracturing. In three specimens, "instantaneous" completion of the initial fracture on one side freed the posterior arch to lengthen its effective lever arm and acquire a lateral tilt as the fracture was slightly displaced temporarily. This transition decreased the angulation and stress in the second side, postponing the second fracture until continued deflection achieved a similar critical angle, now in an oblique (bd) plane.

The two clinical cases confirm that the deflection sometimes stops before the second side of the arch fails. After removal of the traumatic force, the unilateral type of fracture is undisplaced and is splinted by the intact side.

ACKNOWLEDGMENTS

We thank Mark Birchette, Department of Anatomy, Johns Hopkins School of Medicine, for the atlas specimens, and Kenneth Scott and Arnetrice Nealy, Parkland Hospital, Dallas, for specimen radiography.

REFERENCES

1. Gehweiler JA Jr, Osborne RL Jr, Becker RF. *The radiology of vertebral trauma*. Philadelphia: Saunders, 1980:148
2. Plaut HF. Fractures of the atlas resulting from automobile accidents. *AJR* 1938;40:867–890
3. Evans FG. *Mechanical properties of bone*. Springfield, IL: Thomas, 1973:56–60, 123–160